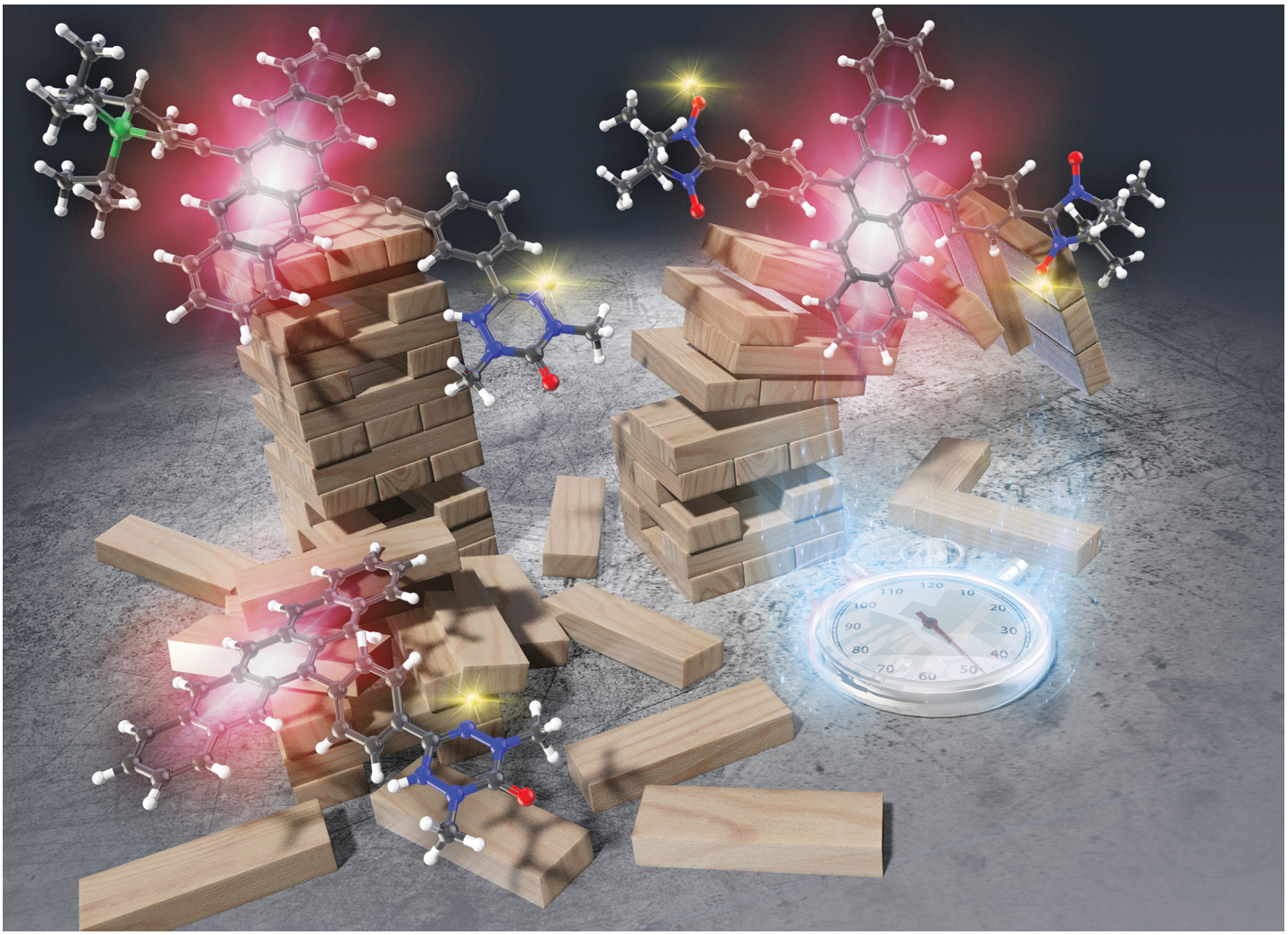

Showing research from Professor Yoshio Teki *et al.* at Osaka City University, Japan

π-Topology and ultrafast excited-state dynamics of remarkably photochemically stabilized pentacene derivatives with radical substituents

Building blocks depict the photochemical stability: π-topologically different Pn derivatives with both π-radical- and TIPS-substituents are synthesized, which showed remarkably improved photochemical stability (at least 10^2 times higher than that of TIPS-Pn). Ultrafast intersystem crossing within sub-pico second for the purely organic compounds is realized without heavy atoms by effective π-conjugation. The relationship between π-topology and the photochemical stability is also discussed based on the excited-state dynamics. A synergetic effect exists between the radical photo-stabilization and TIPS electronic-stabilization.

As featured in:

See Yoshio Teki *et al.*, *Phys. Chem. Chem. Phys.*, 2022, **24**, 13514.

ROYAL SOCIETY OF CHEMISTRY

rsc.li/pccp

Registered charity number: 207890

PCCP

PAPER

View Article Online
View Journal | View Issue

Cite this: *Phys. Chem. Chem. Phys.*, 2022, **24**, 13514

π-Topology and ultrafast excited-state dynamics of remarkably photochemically stabilized pentacene derivatives with radical substituents†

Nishiki Minami,[a] Kohei Yoshida,[a] Keijiro Maeguchi,[a] Ken Kato,[a] Akihiro Shimizu,[a] Genta Kashima,[a] Masazumi Fujiwara,[a] Chiasa Uragami,[b] Hideki Hashimoto [b] and Yoshio Teki *[a]

Received 10th February 2022,
Accepted 8th April 2022

DOI: 10.1039/d2cp00683a

rsc.li/pccp

Pentacene derivatives with both π-radical- and TIPS-substituents (**1*m*** and **1*p***) were synthesized and their photochemical properties and excited-state dynamics were evaluated. The pentacene-radical-linked systems **1*m*** (**1*p***) showed a remarkable improvement in photochemical stability, which was 187 (139) times higher than that of 6,13-bis(triisopropylsilylethynyl)pentacene. Transient absorption spectroscopy showed that this remarkable photostabilization is due to the ultrafast intersystem crossing induced by effective π-conjugation between the radical substituent and pentacene moiety. The relationship between π-topology and the photochemical stability is also discussed based on the excited-state dynamics.

Introduction

Pentacene (Pn) derivatives have been intensively studied as promising candidates for organic field-effect transistors (OFETs),[1] organic thin-film transistors (OTFTs),[2] and organic light-emitting diodes (OLEDs)[3,4] owing to their high hole mobility in the solid state.[5,6] In addition, it is also a promising spin-current transport material that is useful for spintronics.[7,8] Improving the photochemical stability of Pn derivatives is an important issue because the Pn framework easily decomposes by reacting with oxygen under ambient light.[9,10] A typical stabilization methods involves the use of a bulky and/or electron-withdrawing substituent(s) on the Pn moiety,[2,11,12] of which a representative example is 6,13-bis(triisopropylilylethynyl)pentacene (TIPS-Pn) reported by J. E. Anthony *et al.*[10,11] We reported a different strategy for the photochemical stabilization (radical photostabilization) that utilized the unique excited-state spin dynamics induced by the attachment of the π-radical substituent(s) to the Pn moiety.[13–15] Thus, Pn derivatives with one[13] or two[14] π-radical substituent(s) were significantly more stable against photodegradation because of the enhanced/accelerated intersystem crossing (EISC) of the Pn moiety.[15]

In this study, we report the design and synthesis of new Pn derivatives (**1*m*** and **1*p*** in Fig. 1) with both π-radical and TIPS substituents, which have different π-orbital networks (*i.e.*, π-topology). We evaluated their photochemical properties and their excited-state dynamics in the relation to the π-topology. The spin-state ordering and dynamics in the photoexcited states expected according to the spin-density distributions in the pohotoexcited states[16,17] are also shown in Fig. 1 The π-radical-linked Pn derivatives (**1*m*** and **1*p***) showed remarkable improvement in photochemical stability much over the previously reported radical-linked pentacene derivatives (**2**, **3**, and **4**)[13,14] or TIPS-Pn (Fig. 1). This remarkable photochemical stability has been ascribed to the ultrafast (femtosecond) EISC induced by the effective π-conjugation between the radical substituent and the pentacene moiety owing to the molecular planarity.

Results and discussion

1*m* was synthesized from 6,13-pentacenedione as the starting material, according to the procedures shown in Scheme 1. **5** was synthesized from 6,13-pentacenedione according to the similar procedures described in the literature.[18] **6m** was synthesized from **5** by a lithiation reaction with 40% yield and, then, reduced in the dark to **7m** under acidic condition with 74% yield.[19] A condensation reaction of **7m** with 1,3-diamino-1,3-dimethylurea in a $(CH_2Cl)_2$/

[a] *Division of Molecular Materials Science/Department of chemistry, Graduate School of Science, Osaka City University, 3-3-138 Sugimoto, Sumiyoshi-ku, Osaka 558-8585, Japan. E-mail: teki@osaka-cu.ac.jp*
[b] *Department of Applied Chemistry for Environment, Graduate School of Science and Technology, Kwansei Gakuin University, Sanda, Hyogo 669-1337, Japan*

† Electronic supplementary information (ESI) available: Experimental details and supplementary figures. See DOI: https://doi.org/10.1039/d2cp00683a

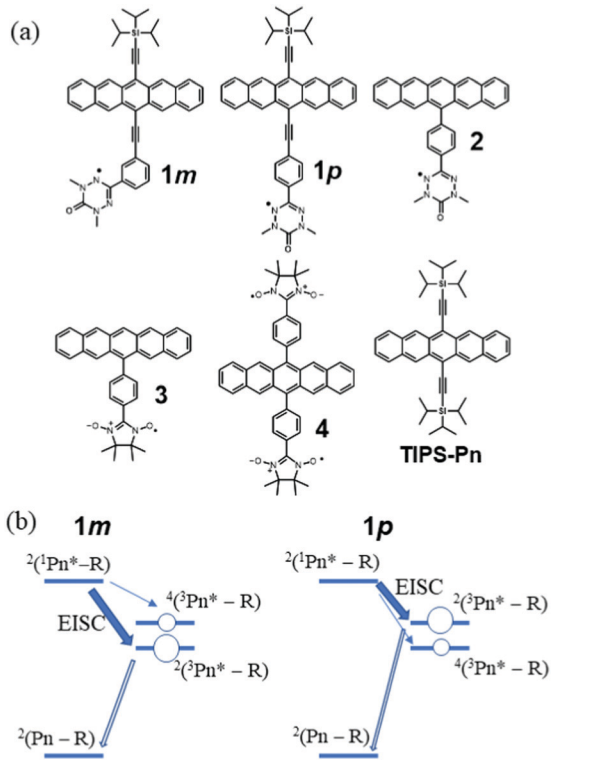

Fig. 1 (a) Chemical structures for π-radical-linked pentacene derivatives (**1*m***, **1*p***, **2**, **3**, and **4**), and TIPS-Pn. (b) Expected excited-state dynamics for **1*m*** and **1*p***.

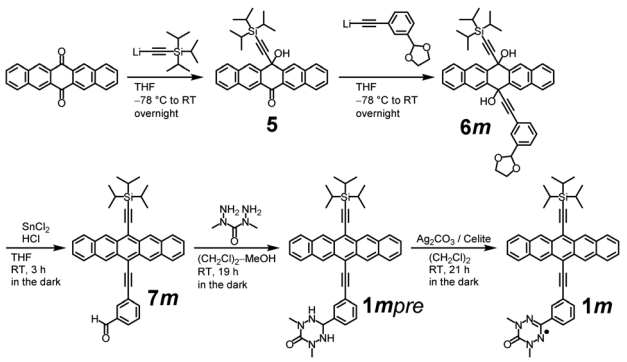

Scheme 1 Synthetic route for **1*m***.

methanol mixture afforded **1*mpre***. Finally, oxidation of **1*mpre*** by Ag_2CO_3 on Celite (48 wt%) produced **1*m*** as a greenish-blue powder after recrystallization (19% yield). **1*p*** was synthesized using similar procedures. The detailed synthetic procedures for **1*m*** and **1*p*** are described in the ESI.†

To characterize the electronic structures of **1*m*** and **1*p***, electron spin resonance (ESR) and cyclic voltammetry (CV) measurements were performed. The obtained and simulated ESR spectra of **1*m*** and **1*p*** are shown in Fig. S13 (ESI†), which was adequately characterized as a dimethyloxoverdazyl radical according to their *g* values and the hyperfine splitting, which are similar to those of the phenyl-dimethyl-substituted

Table 1 Electrochemical (oxidation (Ox) and reduction (Red)), and photochemical stability data of **1*p***, **1*m***, TIPS-Pn, **2**, **3**, and **4** in air-saturated CH_2Cl_2

Derivatives	First redox potentials *vs.* Fc/Fc^+ E[Ox]/V	E[Red]/V	τ_{dec}/hour
1*m*	0.332	−1.32, −1.47	178 ± 6 (97%, dominant) 3.03 ± 0.43 (3%, minor)
1*p*	0.322	−1.32, −1.46	132 ± 4 (96%, dominant) 0.90 ± 0.16 (4%, minor)
TIPS-Pn	0.402	−1.45	0.950 ± 0.015
2	0.294[7,13]	−1.38[13]	0.737 ± 0.014
3	0.298[13]	−1.37[13]	2.64 ± 0.05
4	0.405	−1.24	15.4 ± 0.1

oxoverdazyl radical.[20] The cyclic voltammograms (CV) of **1*m***, **1*p***, TIPS-Pn and **4** are shown in Fig. S14 (ESI†). The CV curves of **2** and **3**[13] are not shown here, but their redox potentials are listed in Table 1, and their photochemical stabilities are discussed later. The first oxidation potential of **1*m*** (**1*p***) is 0.332 V (0.322 V), which is close to the middle between TIPS-Pn (0.402 V) and **2** (0.294 V) or **3** (0.298 V). Notably, the oxidation potential of the verdazyl radical overlaps with that of the pentacene moiety.[21] These findings obtained from the CV data show that the electronic states of the pentacene moiety in their ground state are almost unchanged by the attachment of the radical substituent similar to shown already in our previous work.[13] Although the luminescence of **1*m*** and **1*p*** were completely eliminated by the ultrafast EISC shown later, their ground-state properties of the pentacene moiety are not affected by the radical substituent, leading to the application to OFETs, OTFTs, spintronics devices and so forth. It has been actually shown in our preliminary experiment that **1*p*** acts as the efficient hole transport material in the OFETs (not shown). In addition, the luminescent property of the pentacene is expected to recover by a weak acid treatment after making devices, leading to the possible application for OLEDs.

The photochemical stabilities of **1*m*** and **1*p*** were evaluated by comparing them with TIPS-Pn, **2**, **3**, and **4** in air-saturated CH_2Cl_2 solution at room temperature (*ca.* 20 °C) under irradiation with visible light (light power 70 mW; $\lambda_{ex} = 650 \pm 25$ nm for **1*m***, **1*p*** and TIPS-Pn; $\lambda_{ex} = 600 \pm 25$ nm for **2**, **3** and **4**). The setup of the irradiation system is shown in Fig. S18 (ESI†). Fig. 2a–c show the photoirradiation-induced time-variations in the steady-state absorption spectra of **1*m***, **1*p***, and TIPS-Pn, respectively, in CH_2Cl_2. Only a 13(17)% decrease in the absorbance was observed for **1*m*** (**1*p***) for 20 h, showing their remarkable photochemical stabilities. In contrast, TIPS-Pn, a well-known commercially available photochemically stable pentacene derivative, showed a significant decay of the $^1\pi$–π^* absorption band of the Pn moiety within 2 h. The time variations in the absorption spectra of the other compounds are provided in the ESI.† The $^1\pi$–π^* transition of the Pn moiety in **1*m*** (**1*p***) was observed at the peak wavelength of 653.5 nm (658 nm), which was *ca.* 10.5 (15) nm red-shifted than that for TIPS-Pn. The molar absorption coefficient (ε) of **1*m*** (**1*p***) in CH_2Cl_2 was determined to be 35 600 M^{-1} cm^{-1} at 653.5 nm

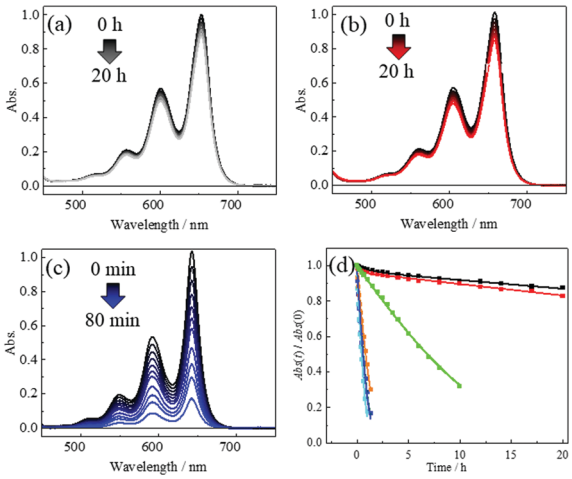

Fig. 2 Photochemical stability of **1*m*** (black), **1*p*** (red), TIPS-Pn (blue), **2** (light blue), **3** (yellowish brown) and **4** (yellow green) in air-saturated CH_2Cl_2 at room temperature. Time variations in the absorption spectra of (a) **1*m***, (b) **1*p***, and (c) TIPS-Pn. (d) Time variations in absorbance of the peaks in 0 ← 0 band for **1*m***, **1*p***, TIPS-Pn, **2**, **3**, and **4**. Their curve fittings were obtained using eqn (1) for TIPS-Pn, **2**, **3**, and **4** or eqn (2) for **1*m*** and **1*p***. Abs(0) values of **1*m***, **1*p***, TIPS-Pn, **2**, **3**, and **4** were 1.001, 1.013,1.035, 1.036, 1.037, and 1.014, respectively.

(38 000 M^{-1} cm^{-1} at 658 nm), which is almost identical to that of TIPS-Pn (ε = 28 900 (27 100) M^{-1} cm^{-1} at 640 nm (643 nm) in THF (CH_2Cl_2)).[14] The n–π transition of the verdazyl radical was masked by the overlap with the $^1\pi$–π^* transition. These characteristics were well reproduced by the TD-DFT calculations (Fig. S19–S21 in ESI†). Fig. 2d shows the decay profiles of the low-energy $^1\pi$–π^* absorption peaks of all compounds studied in this work (**1*m***: λ = 653.5 nm, **1*p***: λ = 658 nm, TIPS-Pn: λ = 643 nm, **2**: λ = 589.5 nm, **3**: λ = 589.5 nm, and **4**: λ = 602 nm). The decay profiles of **2**, **3**, **4** and TIPS-Pn were analyzed by using the following eqn;[14]

$$\mathrm{Abs}(t) = \log_{10}\left\{1 + \frac{10^{\mathrm{Abs}(0)} - 1}{10^{t/\tau_{\mathrm{dec}}}}\right\} \quad (1)$$

where, Abs(t) refers to the absorbance at time t. In this eqn, the decrease in the absorbance at the excitation wavelength by the photochemical reaction of the Pn moiety was considered. The characteristic time (t_{dec}) for the decomposition of the Pn moiety by the photochemical reaction with the molecular oxygen was determined by the least-squares fitting. In the case of **1*m*** and **1*p***, a small amount of impurity (<4%) with a decomposition time comparable to that of TIPS-Pn was present; therefore, their decay profiles were well analyzed using the following eqn;

$$\mathrm{Abs}(t) = \log_{10}\left\{1 + \frac{10^{\mathrm{Abs1}(0)} - 1}{10^{t/\tau 1_{\mathrm{dec}}}}\right\} + \log_{10}\left\{1 + \frac{10^{(\mathrm{Abs}(0)-\mathrm{Abs1}(0))} - 1}{10^{t/\tau 2_{\mathrm{dec}}}}\right\} \quad (2)$$

where, Abs1(0), and $\tau 1_{\mathrm{dec}}$, and {Abs(0) – Abs1(0)}, and $\tau 2_{\mathrm{dec}}$ refer to the initial absorbance and the decay times of the major and minor components, respectively. The $\tau 1_{\mathrm{dec}}$ values for **1*m*** and **1*p*** were 178 ± 6 h and 132 ± 4 h, respectively, which are significantly longer than the decay times of previously reported radical-linked pentacene derivatives (**2**, **3**, and **4**) and TIPS-Pn. The $\tau 2_{\mathrm{dec}}$ values for **1*m*** and **1*p*** were 3.03 ± 0.43 and 0.90 ± 0.16 h, respectively, which are comparable to the decay time of TIPS-Pn (0.950 ± 0.015 h), indicating that these belong to non-radical species having both TIPS and Pn moieties, which are likely to be decomposed products of the radical species. The photochemical stabilization data are summarized in Table 1. Overall, the presence of a radical substituent exerts a remarkable photochemical stability for **1*m*** (**1*p***), which is approximately 187(139), 242(179), and 11.6 (8.6) times higher than that of TIPS-Pn, **2**, and biradical **4** (the most photostable radical-linked pentacene derivative reported previously), respectively. In addition, **1*m*** and **1*p*** can be easily dissolved in the common organic solvents such as CH_2Cl_2, because of the TIPS substituent; the calculated dipole moments of **1*m***, **1*p***, and TIPS-Pn are 0.74, 0.68, and 0.10 Debye, respectively.

We reported that intersystem crossing (ISC) in Pn and anthracene derivatives was enhanced/accelerated by introducing π-radical substituent(s),[15,16,22] and a similar phenomenon was observed for ultrafast ISC for perylene-3,4,9,10-bis-(dicarboximide) derivatives with radical substituent(s).[23,24] The excited singlet states (^{1}Pn*) in **1*m*** and **1*p*** were expected to be efficiently converted to the excited triplet state (^{3}Pn*) by the EISC. Thus, the enhanced/accelerated ISC mechanism in the Pn moiety from ^{1}Pn* to ^{3}Pn* works in **1*m*** and **1*p***, leading to the observed remarkable photochemical stability, because the photochemical reaction of the Pn derivative with oxygen occurs predominantly in ^{1}Pn* states.[25] The enhancement in the photostability was much larger than that of **2**, **3**, **4**, and TIPS-Pn. It should be noted that the increase in the number of radical or TIPS substituents leads to an additional effect on the photostability, which is "linearly" (or close to linearly) proportional to the number of substituents.[13,14,19] Therefore, the significant increase in the photochemical stability of **1*m*** and **1*p*** is due to their molecular planarity, which leads to the ultrafast (enhanced) ISC by the effective π-conjugation between the radical substituent and pentacene moiety. The synergetic effect of the radical photostabilization and the electronic effect of the TIPS substituent may also contribute to this enormous photostability.

To confirm the above speculation and gain further insight into the excited-state dynamics, we performed transient absorption (trA) measurements. The experimental details are described in the ESI.† Fig. 3 shows the color maps of the trA spectra and time courses at the characteristic wavelengths. Typical time courses of the spectra are provided in the ESI.† The transitions at 446 nm and 574 nm in Fig. 3a correspond to the wavelength of the trA peaks of **1*m*** at an early stage, which was assigned to the singlet excited state of the Pn moiety (^{1}Pn*). The peak wavelength of the triplet excited state of the Pn moiety (^{3}Pn*) corresponds to 497 nm, while that of the bleach corresponds to 644 nm (see ESI†). The time-dependent decays of the trA intensities (ΔAbs) at 446 nm and 574 nm were analyzed using a double exponential function ($\Delta\mathrm{Abs}(t) = C_S\exp(-t/\tau_S)$ +

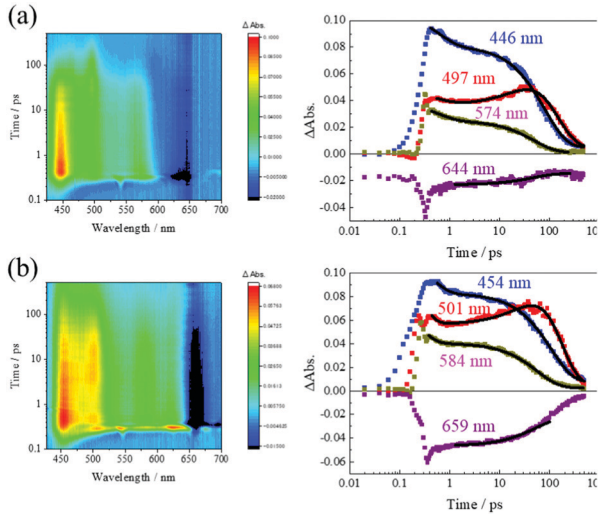

Fig. 3 Typical transient absorption data. (a) **1*m*** (Left: Color maps of the transient absorption spectra. Right: Time decays at the characteristic wavelengths.) (b) **1*p*** (Left: Color maps of the transient absorption spectra. Right: Time decays at the characteristic wavelengths.).

$C_T\exp(-t/\tau_T)$, where, τ_S and τ_T refer to the singlet state and triplet state lifetimes of Pn* moiety, respectively), showing that the trA spectra of ^{1}Pn* and ^{3}Pn* overlapped. It should be noted that the total spin states of the whole molecule are sing-doublet, $^2(^1$Pn*–R) for ^{1}Pn*, and trip-doublet $^2(^3$Pn*–R) and trip-quartet $^4(^3$Pn*–R) for ^{3}Pn*, respectively. Therefore, τ_S and τ_T denote the lifetimes of ^{1}Pn*–R and ^{3}Pn*–R, respectively. The τ_S value was estimated from the fit of the trA decay at 574 nm, where the trA of ^{1}Pn* was the most dominant (the τ_S estimated from the fit of the trA decay at 446 nm was 560 ± 43 fs which was within the experimental error). The recovery of the bleach at 644 nm was used to estimate the average decay time ($\langle\tau_T\rangle$) of ^{3}Pn* because the process related to ^{3}Pn* is slightly complicated, as follows. The trA intensity at 497 nm first decreased, second increased and then decreased, which may suggest the existence of an indirect pathway from ^{1}Pn* to ^{3}Pn* (see ESI†). This behavior is difficult to fit using a simple double exponential function. The triplet lifetime (τ_T) was roughly estimated from the least-squares fit using a triple exponential function (see ESI†). The τ_S and $\langle\tau_T\rangle$ values of **1*p*** were estimated by the double exponential fit of the decay of the TrA peak at 584 nm and by the single exponential fit of the recovery of the bleach at 659 nm in Fig. 3b, respectively. The peak at 584 nm corresponds to the trA peak of **1*p*** (see ESI†) at an early stage. The τ_T value was roughly estimated from the fit using a triple exponential function (see ESI†), because the indirect pathway from ^{1}Pn* to ^{3}Pn* is also indicated from the time course of the trA intensity at 501 nm. The obtained lifetimes (τ_S, τ_T, and $\langle\tau_T\rangle$) are listed in Table 2 along with the lifetimes (τ_S and τ_T) of **2**, **3** and TIPS-Pn. The lifetimes of the precursors (**1*m***pre and **1*p***pre) were similar to those of the TIPS-Pn (see ESI†).

The τ_S of **1*m*** (**1*p***) was *ca.* 1.8×10^4 (7.0×10^4) times shorter than that of TIPS-Pn because of the EISC and 35 (140) times shorter than that of **2** due to the effective π-conjugation, as a result of the molecular planarity (the dependency on the radical species was less than 4 times judging from the τ_S of **2** and **3**). The $\langle\tau_T\rangle$ of **1*m*** (**1*p***) was *ca.* 8.8×10^4 (5.8×10^4) times shorter than τ_T of TIPS-Pn and 17 (11) times shorter than that of **2** (On the discussion related to the photochemical stability, $\langle\tau_T\rangle$ is better than τ_T.). It is known that the difference in the exchange-couplings between the unpaired electron on the radical and the electrons in half-filled orbitals on the excited chromophore is important in the EISC rather than the magnitude of the exchange coupling,[26,27] although the effective π-conjugation is expected to be one of the critical factors in EISC of **1*m*** and **1*p***. The detailed discussions of the expected mechanism for the ultrafast quenching of the photoexcited states is described in the ESI.† Because the photochemical stability of **1*m*** (**1*p***) is 242(179) times higher than that of **2**, a synergetic effect between the radical photo-stabilization and TIPS electronic stabilization seems to exist, but the dominant effect is due to the ultrafast EISC owing to the effective π-conjugation. It should be noted that τ_T and $\langle\tau_T\rangle$ of **1*m*** are shorter than those of **1*p***, which is consistent with the spin-state ordering of $^2(^3$Pn*–R) and $^4(^3$Pn*–R). Thus, as shown in Fig. 1b, the expected lowest excited state of **1*m*** is $^2(^3$Pn*–R) with a low-lying higher energy $^4(^3$Pn*–R) state. Therefore, the spin-allowed transition to the ground-state is expected to occur efficiently from $^2(^3$Pn*–R). In contrast, the expected lowest excited state of **1*p*** is $^4(^3$Pn–R), from which the transitions to the ground state can occur indirectly *via* the low-lying higher-energy $^2(^3$Pn*–R) state. This indicates that the excited-state dynamics can be controlled by π-topology. Notably, the photochemical stability of **1*m*** was higher than that of **1*p***, although the τ_S of **1*p*** was shorter than that of **1*m***. This is understandable as the complete suppression of the reaction pathway *via* ^{1}Pn* is due to the extremely short τ_S value for **1*m*** and **1*p***, although the dominant decomposition pathway of pentacene is known to occur *via* ^{1}Pn*.[28] Thus, the remaining effective decomposition pathways occur in ^{3}Pn*.

Table 2 Lifetimes (τ_S and τ_T) of the singlet and triplet states of the Pn moiety of **1*p***, **1*m***, **2**, **3**, and TIPS-Pn in CH_2Cl_2

	1*m*	**1*p***	**2**[15]	**3**[15]	TIPS-Pn[b]
τ_S	537 fs (37 fs)[a]	135 fs (26 fs)[a]	19 ps	5.3 ps	9.46 ns (0.05 ns)
τ_T	128 ps (3 ps)[a]	163 ps (2 ps)[a]	830 ps	560 ps	4.31 μs (0.32 μs)
$\langle\tau_T\rangle$	49 ps (1 ps)[a]	74 ps (2 ps)[a]			—[c]

[a] Standard error of fit. [b] See ref. 30. [c] Bleach was difficult to separate from the scattered light.

Conclusions

A remarkable improvement in photochemical stability of **1*m*** (**1*p***) was achieved, which was 187 (139), 242(179), and 11.6 (8.6) times higher than that of TIPS-Pn, **2**, and **4**, respectively. It is also worthy of notice that the intersystem crossing of the purely organic compounds without heavy atoms is realized in the sub-femtosecond region. The trA spectroscopy clarified that the ultrafast enhanced/accelerated ISC was realized owing to the

effective π-conjugation between the radical and the pentacene moieties. In contrast, no enhanced/accelerated ISC and no photochemical stability improvement were reported for the Pn derivative attached to the TEMPO radical.[19,29] The strong conjugation of the π-radical with the Pn moiety is essential for the enormous photochemical stabilization of **1*m*** and **1*p***. In addition, π-topological control of the excited-state dynamics was realized and applied to the enhancement of photochemical stability.

Conflicts of interest

There are no conflicts to declare.

Acknowledgements

This work was financially supported by the Grant-in-Aid for Scientific Research (B) (No. 16H04136, No. 20H02715) and Grant-in-Aid for Challenging Exploratory Research (No. 18K19062) from the Japan Society for the Promotion of Science (JSPS). The authors acknowledge to Ms Yumi Umehara (Research Assistant at the Osaka City University) for the help with the sample purification.

Notes and references

1 J. E. Anthony, *Angew. Chem., Int. Ed.*, 2008, **47**, 452.
2 S. K. Park, T. N. Jackson, J. E. Anthony and D. A. Mourey, *Appl. Phys. Lett.*, 2007, 91.
3 M. A. Wolak, B. B. Jang, L. C. Palilis and Z. H. Kafafi, *J. Phys. Chem. B*, 2004, **108**, 5492.
4 M. A. Wolak, J. Delcamp, C. A. Landis, P. A. Lane, J. Anthony and Z. Kafafi, *Adv. Funct. Mater.*, 2006, **16**, 1943–1949.
5 O. D. Jurchescu, J. Baas and T. M. Palstra, *Appl. Phys. Lett.*, 2004, **84**, 3061.
6 J. L. Bredas, D. Beljonne, V. Coropceanu and J. Cornil, *Chem. Rev.*, 2004, **104**, 4971.
7 Y. Tani, Y. Teki and E. Shikoh, *Appl. Phys. Lett.*, 2015, 107.
8 Y. Tani, T. Kondo, Y. Teki and E. Shikoh, *Appl. Phys. Lett.*, 2017, **110**, 032403.
9 I. Lewis and L. Singer, *J. Phys. Chem.*, 1981, **85**, 352.
10 A. Maliakal, K. Raghavachari, H. Katz, E. Chandross and T. Siegrist, *Chem. Mater.*, 2004, **16**, 4980.
11 J. E. Anthony, D. L. Eaton and S. R. Parkin, *Org. Lett.*, 2002, **4**, 15–18.
12 S. S. Palayangoda, R. Mondal, B. K. Shah and D. C. Neckers, *J. Org. Chem.*, 2007, **72**, 6584.
13 Y. Kawanaka, A. Shimizu, T. Shinada, R. Tanaka and Y. Teki, *Angew. Chem., Int. Ed.*, 2013, **52**, 6643.
14 A. Shimizu, A. Ito and Y. Teki, *Chem. Commun.*, 2016, **52**, 2889–2892.
15 A. Ito, A. Shimizu, N. Kishida, Y. Kawanaka, D. Kosumi, H. Hashimoto and Y. Teki, *Angew. Chem., Int. Ed.*, 2014, **53**, 6715.
16 Y. Teki, S. Miyamoto, M. Nakatsuji and Y. Miura, *J. Am. Chem. Soc.*, 2001, **123**, 294.
17 Y. Teki, T. Toichi and S. Nakajima, *Chem. – Eur. J.*, 2006, **12**, 2329.
18 D. Lehnherr, R. McDonald and R. R. Tykwinski, *Org. Lett.*, 2008, **10**, 4163.
19 E. T. Chernick, R. Casillas, J. Zirzlmeier, D. M. Gardner, M. Gruber, H. Kropp, K. Meyer, M. R. Wasielewski, D. M. Guldi and R. R. Tykwinski, *J. Am. Chem. Soc.*, 2015, **137**, 857.
20 F. A. Neugebauer and H. Fischer, *Angew. Chem., Int. Ed. Engl.*, 1980, **19**, 724.
21 J. B. Gilroy, S. D. McKinnon, B. D. Koivisto and R. G. Hicks, *Org. Lett.*, 2007, **9**, 4837.
22 K. Kanemoto, A. Fukunaga, M. Yasui, D. Kosumi, H. Hashimoto, H. Tamekuni, Y. Kawahara, Y. Takemoto, J. Takeuchi, Y. Miura and Y. Teki, *RSC Adv.*, 2012, **2**, 5150.
23 E. M. Giacobbe, Q. Mi, M. T. Colvin, B. Cohen, C. Ramanan, A. M. Scott, S. Yeganeh, T. J. Marks, M. A. Ratner and M. R. Wasielewski, *J. Am. Chem. Soc.*, 2009, **131**, 3700.
24 S. Yeganeh, M. R. Wasielewski and M. A. Ratner, *J. Am. Chem. Soc.*, 2009, **131**, 2268.
25 W. Fudickar and T. Linker, *J. Am. Chem. Soc.*, 2012, **134**, 15071.
26 R. L. Ake and M. Gouterman, *Theor. Chim. Acta*, 1969, **15**, 20.
27 B. W. Stein, C. R. Tichnell, J. Chen, D. A. Shultz and M. L. Kirk, *J. Am. Chem. Soc.*, 2018, **140**, 2221.
28 A. R. Reddy and M. Bendikov, *Chem. Commun.*, 2006, 1179.
29 C. E. Avalos, S. Richert, E. Socie, G. Karthikeyan, G. Casano, G. Stevanato, D. J. Kubicki, J. E. Moser, C. R. Timmel, M. Lelli, A. J. Rossini, O. Ouari and L. Emsley, *J. Phys. Chem. A*, 2020, **124**, 6068.
30 B. J. Walker, A. J. Musser, D. Beljonne and R. H. Friend, *Nat. Chem.*, 2013, **5**, 1019.

